

Article

Lp16-PSP, a member of YjgF/YER057c/UK114 Protein Family Induces Apoptosis and p21^{WAF1/CIP1} mediated G₁ Cell Cycle Arrest in Human Acute Promyelocytic Leukemia (APL) HL-60 Cells

Thomson Patrick Joseph^{1†}, Warren Chanda^{1†}, Abdullah Faeer Muhammad², Sadia Kanwal³, Samana Batool¹, Meishan Zhang¹, MinTao Zhong¹ and Min Huang^{1*}

¹Department of Microbiology, College of Basic Medical Sciences, Dalian Medical University, Dalian, Liaoning 116044, China

²Institute of Cancer Stem Cell, Dalian Medical University, Dalian, Liaoning 116044, China

³Department of Biotechnology, College of Basic Medical Sciences, Dalian Medical University, Dalian, Liaoning, China

[†]Contributed Equally

*Corresponding Author: huangminchao@163.com; +8641186110304

Abstract:

Lp16-PSP from *Lentinula edodes* strain C₉₁₋₃ has been reported previously in our laboratory to have selective cytotoxic activity against a panel of human cell lines. Herein, we have used several parameters in order to characterize the Lp16-PSP-induced cell death using HL-60 as model cancer. The results of phase contrast microscopy, nuclear examination, DNA fragmentation detection and flow cytometry revealed that high doses of Lp16-PSP resulted in the induction of apoptosis in HL-60 cells. The colorimetric assay showed the activation of caspase-8, -9 and -3 cascade highlighting the involvement of Fas/FasL-related pathway. Whereas, western blot revealed the cleavage of caspase-3, increased expression of Bax, the release of cytochrome c and decreased expression of Bcl-2 in a dose-dependent manner, suggesting the intrinsic pathway might be involved in Lp16-PSP-induced apoptosis either. Low doses of Lp16-PSP resulted in the anchorage-independent growth inhibition, induction of G₁ phase arrest accompanied by the increased expression of p21^{WAF1/CIP1} along with the decreased expression of cyclin D, E, and cdk6. Our findings suggest that induction of apoptosis and p21^{WAF1/CIP1} mediated G₁ arrest might be one of the mechanisms of the action of Lp16-PSP, however, further investigations on multiple leukemia cell lines and *in vivo* models are of ultimate need.

Keywords: *Lentinula edodes*; Lp16-PSP; Acute Promyeloid Leukemia; Extrinsic and Intrinsic Apoptotic Pathway; G₁ Phase Cell Cycle Arrest

1. Introduction:

In the United States, approximately after every three minutes, a person is diagnosed with hematological cancer [1]. Leukemia is one of the types of blood cancer that usually initiates in blood-forming organs including bone marrow, followed by the increment in abnormal leukocytes numbers. On the basis of pathological features, leukemia can be classified as acute and chronic leukemia. Where acute leukemia can be acute myeloid leukemia (AML) or acute lymphoblastic leukemia (ALL), and on the other hand chronic leukemia can be chronic myeloid leukemia (CML) or chronic lymphocytic leukemia (CLL) [2]. As far as acute myeloid leukemia (AML) is concerned it is characterized by the malignant hematopoietic progenitor cells (HPCs) accumulation that have impaired differentiation program [3]. In the United States alone, around 21,380 new cases of acute myeloid leukemia (AML) are expected to occur in the year 2017 with an overall five-year survival rate of 26.9% [1].

Acute promyeloid leukemia (APL) is the clear subtype of AML, that is caused by the leukocyte differentiation arrest at the promyelocyte stage and was considered as fatal before the discovery of all-trans retinoic acid (ATRA) the derivative of vitamin A [4]. In the treatment of APL patients, risk stratification is considered to be crucial, and so less intensive regimens are adapted for treating the patients at low risk having white blood cell count (WBC) of $\leq 10,000/\mu\text{l}$, in comparison with patients presenting high-risk disease (WBC $410,000/\mu\text{l}$). Initially, APL patients were defined as low risk for relapse (WBC $\leq 10,000/\mu\text{l}$ and platelet count $440,000/\mu\text{l}$), intermediate risk (WBC $\leq 10,000/\mu\text{l}$ and platelet count $\leq 40k$), and high risk (WBC $410,000/\mu\text{l}$) on the basis of cell count [5]. But because, low- and intermediate-risk patients have common outcomes, and so they were collectively considered as a low-risk disease. As far as therapy for newly diagnosed APL patients is concerned, in the last two decades, it has excogitated from an all-trans retinoic acid (ATRA) + chemotherapy to the arsenic trioxide (ATO) addition followed by the chemotherapy omission in low-risk patients [6].

Natural products, from higher plants, fungi, and microorganisms have a long history of being used as therapeutic agents for the treatment of several diseases. The compounds from natural resources have proven their therapeutic role in unmodified form as well as in contributing a variety of derivatives called secondary metabolites [7]. Concerning the role of natural products in the treatment of leukemia, L-asparaginase, daunorubicin, and the anthracyclines are well-known for their anti-leukemia activities [8]. Successful treatment of the disease not just depends on the category, but also on the genetic factors associated with each disease. Chemotherapy, radiation therapy, antibiotics usage, transfusion and transplantation of blood and bone marrow are some of the strategies used in combination to treat leukemia patients respectively. Although these strategies resulted in prolonged survival, however, some of these treatments are difficult to handle [9]. In order to make advances in our journey toward curative therapy, there is a continuous need of identifying the novel protective mechanisms and pathways responsible for the survival of tumor, as we can not only rely on the presently available arsenals.

In general, if we look into the strategies for combating cancer, in the flow of genetic information, the expression of the gene (s) in the cancer cells can be controlled at different levels, but the drug that targets DNA have the disadvantage of being mutagenic. In contrast, the agents that target RNA are significantly effective without having genotoxic effects [10]. Current strategies to combat cancer are not always effective,

because of the development of resistance, severe side effects, and diversity of the target in the cancer cells. The cancer biologists are targeting the RNA pool of cancer cells as alternative strategies for combating cancer, as it differs significantly from the normal cells highlighting the additive advantage of selective toxicity. In this regard, many of the characterized ribonucleases from various organisms have displayed antitumor activities [11-14] and efforts to increase such arsenals are still ongoing, especially with the natural resources.

Keeping in mind this alternative strategy to combat cancer and based on the bioinformatics analysis, our laboratory has demonstrated that Lp16-PSP from one of the edible mushroom *Lentinula edodes* C₉₁₋₃ is an endoribonuclease L-PSP and is a member of highly conserved YjgF/YER057c/UK114 protein family. Furthermore, we demonstrated the selective anticancer activity of Lp16-PSP against a panel of human cell lines and acute promyeloid leukemia HL-60 cell line was identified as the most sensitive cell line with the IC_{50} value of 74.4 ± 1.07 μ g/ml after 48 h treatment [15]. Therefore, the objective of this study is to use human acute promyeloid leukemia (HL-60 cells) as model cancer to further investigate the potential molecular mechanism of the action of Lp16-PSP. We thus investigated several parameters such as DNA fragmentation, mitochondrial membrane potential, *Bax/Bcl-2* expression, activation of caspases, and cell cycle distribution, in HL-60 cells as *in vitro* model system. In this study, we observed that Lp16-PSP resulted in the increased expression of *FasL*, together with the loss of mitochondrial membrane potential and the release of cytochrome c, indicating that extrinsic and intrinsic pathway might be involved in the induction of apoptosis. Furthermore, Lp16-PSP also resulted in the anchorage-independent growth inhibition and p21^{WAF1/CIP1} mediated G₁ cell cycle arrest in HL-60 cells.

2. Results:

2.1 Lp16-PSP causes cytotoxicity and suppresses the anchorage-independent colony formation of HL-60 cells: After treatment of the HL-60 cells with indicated concentrations of Lp16-PSP, phase contrast images were taken. As shown in Figure. 1A treated HL-60 in comparison with the untreated group, showed an obvious change in morphology, cell volume and size. The cells in the treated group are smaller in size and also showing the cellular bleeding. All these signs indicated that the HL-60 cells are going through the process of apoptosis or are dead. These findings highlighted the implication of Lp16-PSP as a potential anticancer agent against acute promyeloid leukemia (APL).

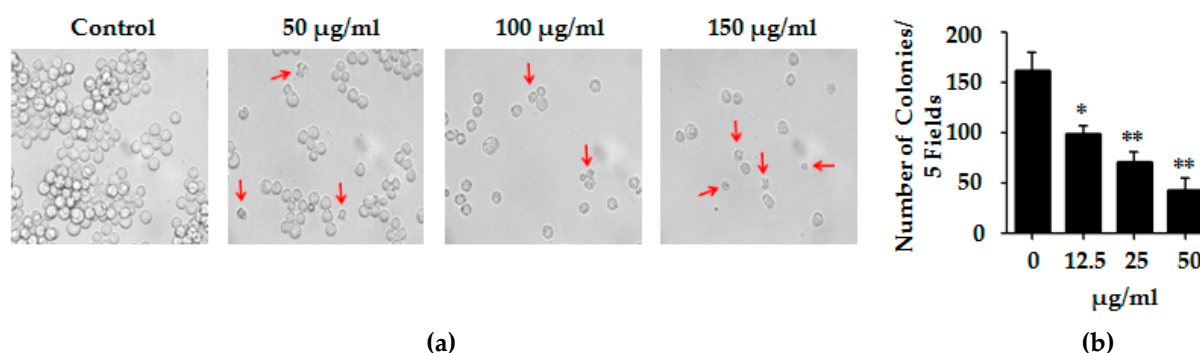
Metastatic malignant cells have the ability to resist the detachment-induced death, which helps them to grow and survive during the period of their dissemination [16]. The HL-60 has been reported previously to have the outstanding property of proliferating and forming sizable colonies in soft agar from a single cell [17]. In order to determine whether Lp16-PSP can affect the HL-60 colony formation, HL-60 cells were mixed with soft agar and cultured till the development of visible colonies. Colonies so formed in the agar were counted carefully. Our results indicated the significant dose-dependent effect of Lp16-PSP on HL-60 colony formation in semisolid agar. These results also indicate that Lp16-PSP treatment resulted in the suppression of HL-60 colony formation without any apparent cytotoxicity at the concentrations of Lp16-PSP used (Fig. 1B).

2.2 Lp16-PSP-Induced Apoptosis in acute promyeloid leukemia (APL) HL-60 cells: Apoptosis or programmed cell death is characterized by certain typical features i.e. shrinkage of the cell, condensation of nuclear chromatin, cleavage of chromosomes, blebbing of membrane and formation of apoptotic bodies [18,19].

In this study, Hoechst 33258 assay was used to monitor changes in the nucleus of HL-60 cells induced after treated with Lp16-PSP. Hoechst 33258 is a DNA-specific fluorochrome which upon excitation with UV emits a blue fluorescence. As shown in Figure. 1C, the nuclei of untreated HL-60 cells are round with homogenous blue fluorescence. Whereas, Lp16-PSP exposed cells showed shrinkage, nuclear chromatin condensation, and apoptotic body formation. The oligonucleosomal fragmentation of chromosomal DNA is another biochemical feature of apoptosis [20-22] that was studied by using DNA fragmentation assay after Lp16-PSP treatment of HL-60 cells for 48 h. DNA was extracted from HL-60 cells and studied using agarose gel electrophoresis. The electrophoretogram given is showing the fragmentation of DNA, while no significant "DNA ladder-like" pattern was found in the control group (Fig. 1D). Moreover, a concentration-dependent increase in DNA cleavage was also observed for the Lp16-PSP treated samples.

Another hallmark of apoptosis is the externalization of phosphatidylserine on the cell membrane prior to the loss of cell membrane integrity [19,23], which can be monitored by annexin V/propidium iodide (AV/PI) staining [24,25]. HL-60 cells after treatment with various concentrations (0 $\mu\text{g/ml}$, 50 $\mu\text{g/ml}$, 100 $\mu\text{g/ml}$ and 150 $\mu\text{g/ml}$) of Lp16-PSP for 48 h were analyzed for the induction of apoptosis by using annexin V/propidium iodide (AV/PI) staining. After 48 h treatment, the percentage of apoptotic cells (including early and late apoptotic cells) increased with the concentration of Lp16-PSP from 3.51 % to 45.61 % (Fig. 1E). Statistical analysis showed that the percentage of cells in late apoptosis stage was significantly higher than the control group upon Lp16-PSP (100 $\mu\text{g/ml}$ and 150 $\mu\text{g/ml}$) treatment for 48 h. These results suggested that the HL-60 cell death by Lp16-PSP is through the induction of apoptosis.

Figure 1



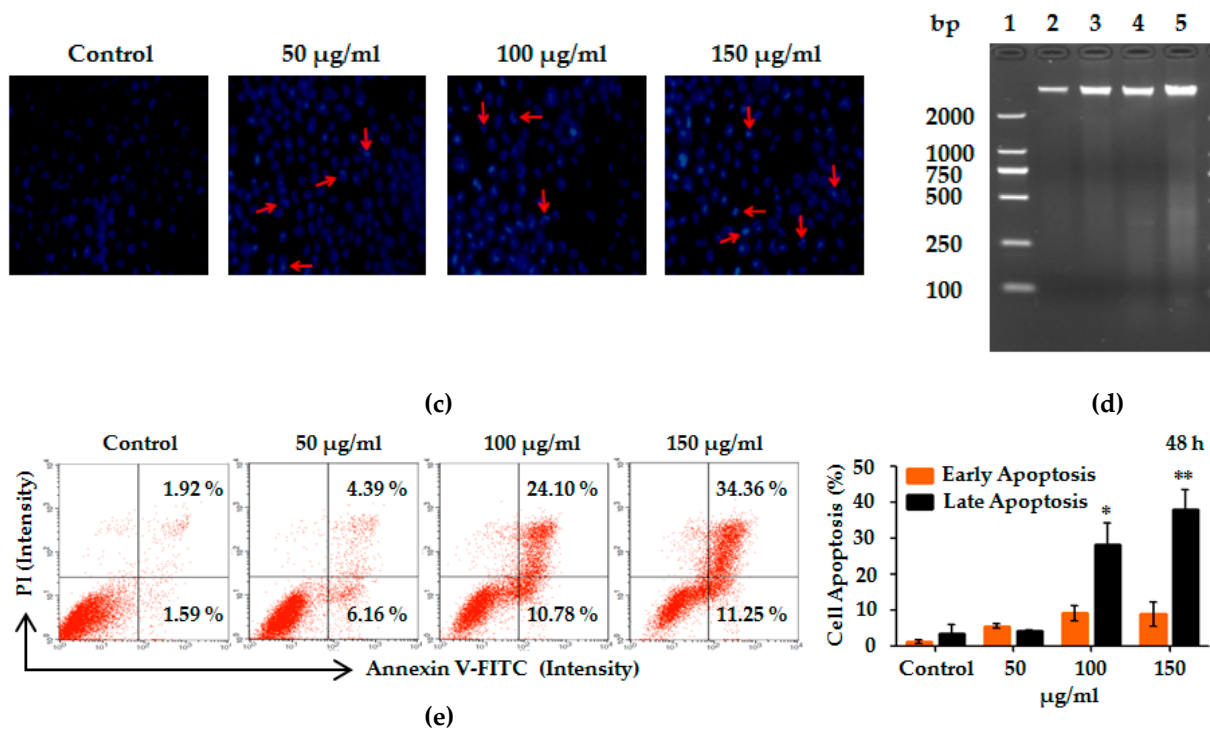


Figure 1: Lp16-PSP-induced apoptosis in acute promyeloid leukemia (HL-60 cells). (a) Phase contrast image of HL-60 cells, untreated and treated samples after 48 h of Lp16-PSP treatment. Red arrowheads are indicating the cells smaller in size and also showing cellular bleeding. (b) Effect of different concentration of Lp16-PSP (0 µg/ml, 12.5 µg/ml, 25 µg/ml and 50 µg/ml) on colony formation (anchorage-independent growth) of HL-60 cells was evaluated and a number of colonies were counted as described in Materials and methods. The data reported here is the mean ± SD of two separate experiments, * $p < 0.05$, ** $p < 0.01$. (c) Fluorescent images of Hoechst 33258 stained HL-60 cells for nuclear morphological changes after 48 h of Lp16-PSP treatment with indicated concentrations. (d) DNA fragmentation of HL-60 cells treated with 0 µg/ml, 50 µg/ml, 100 µg/ml and 150 µg/ml of Lp16-PSP for 48 h. Lane 1: DNA marker DL2000, Lane 2: 0 µg/ml, Lane 3: 50 µg/ml, Lane 4: 100 µg/ml, and Lane 5: 150 µg/ml Lp16-PSP exposed group. (e) Apoptosis was analyzed by Annexin-V/PI staining after 48 h treatment of HL-60 cells with indicated concentrations of Lp16-PSP. Left, results as histogram from one representative experiment treated with 0 µg/ml, 50 µg/ml, 100 µg/ml and 150 µg/ml of Lp16-PSP after 48 h treatment. The lower left (Annexin V-/PI-) and lower right (Annexin V+/PI-) quadrants are showing the viable cell population and the cells at the early apoptosis respectively, and the upper-right quadrant (Annexin V+/PI+) is showing the cell population at the late apoptosis. Right, a number of cells in early and late apoptotic phase were calculated. The data are expressed as mean ± SD (* $p < 0.05$, ** $p < 0.01$).

2.3 Involvement of extrinsic and intrinsic pathways in the Lp16-PSP induced apoptosis: Apoptosis occurs through two main pathways: the Fas death receptor-triggered extrinsic pathway [26] and the mitochondrial-mediated or intrinsic pathway [27]. The initiator caspases i.e. caspase-8 and -9, upon activation, causes the activation of caspase-3, -6, and -7 which results in the cleavage of the cytoskeleton and nuclear protein, ultimately leading to apoptosis [28]. Bcl-2 family of proteins that also play a central role in intrinsic apoptosis pathway by binding with Bax and preventing the mitochondrial pore formation and the release of cytochrome c [29]. On the other hand, pro-apoptotic Bax expression causes the induction of apoptosis [30]. So, in order to characterize the Lp16-PSP induced apoptosis, we evaluated various

apoptosis-related genes such as *Bax*, *Bcl-2*, *Caspase-3*, *Caspase-8*, *Caspase-9*, and *FasL* after treatment with Lp16-PSP by using qRT-PCR. Treatment with Lp16-PSP (IC_{50} concentration) resulted in the significant up- and down-regulation of *FasL* and *Bcl-2* transcripts respectively, together with increased expression of *Bax*, *Caspase-3*, -8 and -9 (Fig. 2A, and 3B). Furthermore, the activation of caspase-8 and -9 (initiator caspases) and caspase-3 (effector caspase) was confirmed by the colorimetric assay performed after 48 h of treatment with different concentrations of Lp16-PSP which showed the activation of caspase-8, -9 and -3 in a dose-dependent fashion (Fig. 2B). In addition, western blot analysis also revealed the cleavage of caspase-3 and the dose-dependent increase and decrease in the expression of Bax and Bcl-2 proteins respectively (Fig. 2C). Increased expression of Bax results in the increased cytochrome c release, that is associated with the mitochondrial damage and intrinsic pathway [31]. In our study, Lp16-PSP has resulted in the significant mitochondrial membrane potential loss which ultimately resulted in the release of cytochrome c from mitochondria into the cytosol (Fig. 2D, 2E). All these findings suggest that Lp16-PSP have triggered both extrinsic and intrinsic apoptosis pathway, however, a detailed investigation is required to further characterize the Lp16-PSP induced apoptosis in terms of signal transduction pathway (s) responsible for these outcomes.

Figure 2

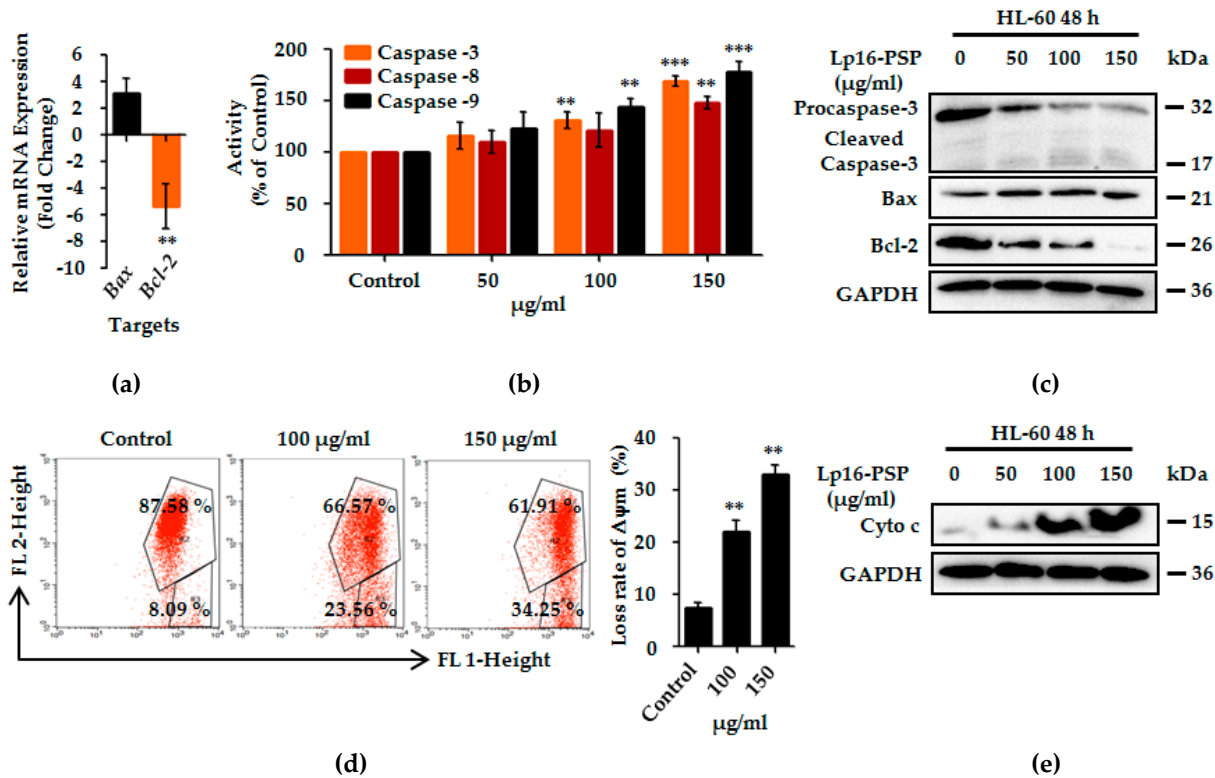


Figure 2: Involvement of Extrinsic and Intrinsic Pathway in Lp16-PSP-induced Apoptosis. (a) Effect of Lp16-PSP on the expression of *Bax* a pro-apoptotic and *Bcl-2* an anti-apoptotic genes, after 48 h of treatment, as evaluated by qRT-PCR. The mRNAs under investigation from the test was normalized to GAPDH and plotted as fold change to the mRNA of control untreated cells, defined as 1. The data expressed here are mean \pm SD of the three individual

experiments (** $p < 0.01$). (b) The colorimetric analysis of caspase-3, -8, and -9 after treatment with an indicated concentration of Lp16-PSP for 48 h. The data reported here are the mean \pm SD of three independent experiments each performed in triplicate (** $p < 0.01$, *** $p < 0.001$). (c) Western blot analysis of the cleavage of caspase-3, Bax, and Bcl-2 after treatment with different concentrations (0 $\mu\text{g/ml}$, 50 $\mu\text{g/ml}$, 100 $\mu\text{g/ml}$ and 150 $\mu\text{g/ml}$) of Lp16-PSP for 48 h, using GAPDH as an internal control. (d) The loss of mitochondrial membrane potential in HL-60 cells after treatment with indicated concentrations of Lp16-PSP for 48 h. Left, results from one representative experiment of HL-60 cells treated with indicated concentrations of Lp16-PSP. Right, the loss rate of mitochondrial membrane potential as compared with the control. The data reported here are mean \pm SD (** $p < 0.01$). (e) The release of cytochrome c detected by western blotting after treatment with indicated concentrations of Lp16-PSP for 48 h, using GAPDH as an internal control.

2.4 Lp16-PSP Induces G₁ Phase Cell Cycle Arrest in HL-60 cells: Lp16-PSP resulted in the suppression of HL-60 cell growth in a dose- and time-dependent fashion [15]. In order to verify that the suppression of growth is due to the disruption of the cell cycle, flow cytometry was done for the analysis of cell cycle distribution after Lp16-PSP treatment at different concentrations (0 $\mu\text{g/ml}$, 25 $\mu\text{g/ml}$, and 50 $\mu\text{g/ml}$). As shown in Figure. 3A, Lp16-PSP treatment at low doses i.e. 25 $\mu\text{g/ml}$ or 50 $\mu\text{g/ml}$ resulted in an increased cell population in G₁ phase, with approximately 49 % and 60 % cells in G₁ phase respectively, in comparison to approximately 32 % in control after 48 h treatment. This increase G₁ phase cell population was observed to be related to the decrease in the S phase population, however upon treatment G₂/M phase remained unchanged. These findings suggest that Lp16-PSP at low doses caused HL-60 growth suppression by modulating the progression of cell cycle without the induction of apoptosis.

2.5 Lp16-PSP induced p21^{WAF1/CIP1} mediated G₁ cell cycle arrest in HL-60: Furthermore, we investigated the effect of Lp16-PSP on different cell cycle regulatory gene at mRNA and protein levels after 48 h of treatment. As p21 is well-recognized as the universal inhibitor of cyclin-cdk complexes [32-34] we assessed the expression of p21, and p27, cyclins (cyclin D1, cyclin E1) and cdks (cdk2, cdk4, cdk6) that are operative in the G₁ phase of the cell cycle by qRT-PCR. Treatment of HL-60 cells with Lp16-PSP (IC_{50} concentration) resulted in the down-regulation of *cdk2*, *cdk4*, *cdk6*, *cyclin D1* and *cyclin E1*, with the significant up-regulation of *CDK inhibitory genes (p21)*, however, increased expression of *p27* was also observed (Fig. 3B). Moreover, Western blotting revealed the dose-dependent decrease and increase in the expression of cdk6, cyclin D1, cyclin E1 and p21 respectively (Fig. 3C). Therefore, these results suggested that proliferation inhibition and G₁ arrest in HL-60 is mediated by the upregulation of p21 that is involved in the progression of the cell cycle from the G₁-S phase.

It has been uncovered by the molecular analysis of human tumors that cell cycle controllers are often mutated in the majority of the malignancies thus the control of cell cycle progression in cancer is thought to be one of the compelling strategies to battle cancer [35,36]. Our data suggested the potential application of Lp16-PSP in combating cancers with deregulated cell cycle components.

Figure 3

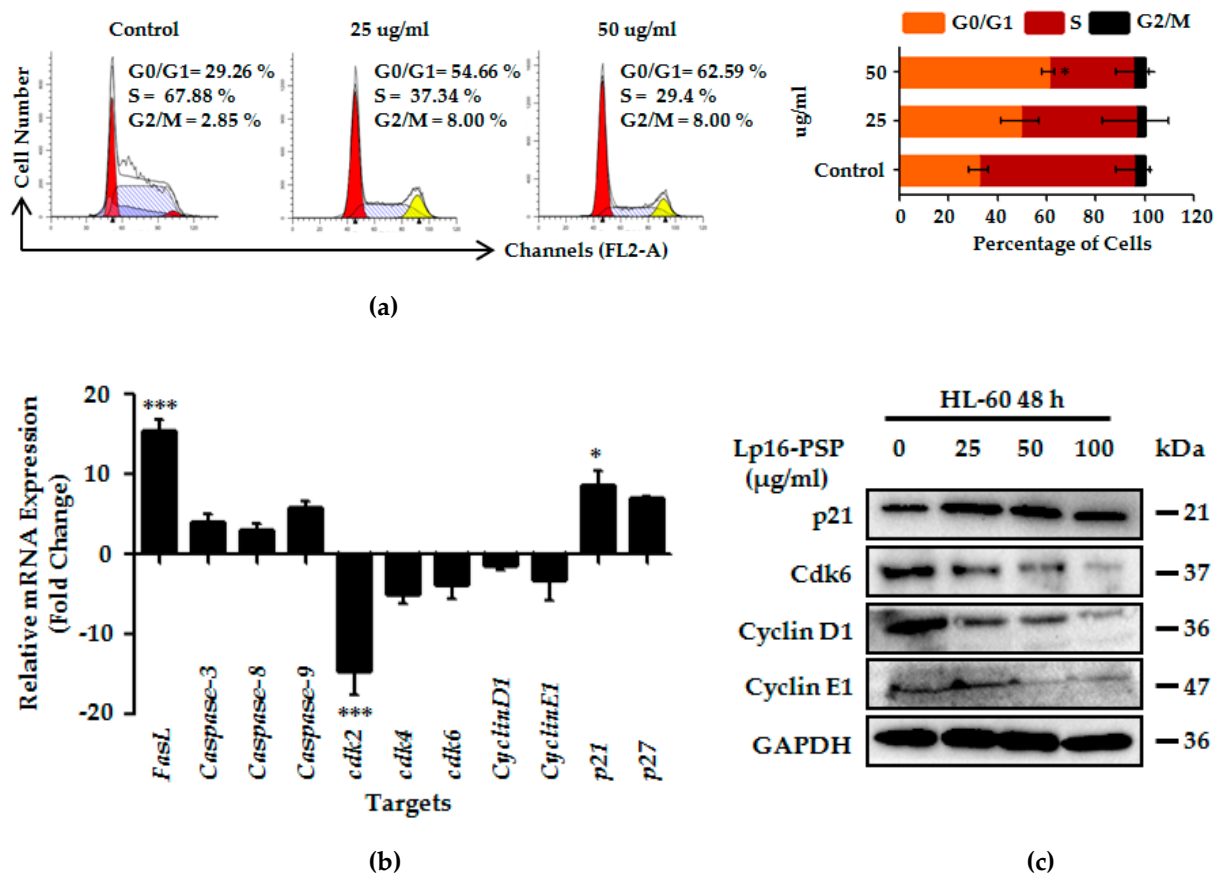


Figure 3: Lp16-PSP-Induced p21^{WAF1/CIP1} mediated G₁ Cell Cycle Arrest in HL-60 Cells. (a) HL-60 cells untreated and treated with various concentrations of Lp16-PSP for 48h were analyzed for DNA content using flow cytometry. Left, results of the one representative experiment indicating the distribution and percentages of cells in G₀/G₁, S and G₂/M phase. Right, is the graphical presentation of the distribution and percentages of cells in different phases of cell cycle. The data presented here is mean \pm SD where * p <0.05. (b) qRT-PCR analysis of apoptosis- and cell cycle-related genes. The data presented here is the mean \pm SD of two independent experiments each run in triplicate. Where * p <0.05, *** p <0.001. (c) Western Blot of cell cycle-related proteins after Lp16-PSP treatment with indicated concentrations for 48 h. GAPDH was used as internal control.

3. Discussion: We have reported the cloning, expression and selective *in vitro* anticancer activity of Lp16-PSP from *L. edodes* strain C₉₁₋₃ against a panel of human cancer and normal cell lines and HL-60 cell line was identified as one of the most sensitive cell lines used [15]. So, for further investigations, we have used human acute promyeloid leukemia (HL-60 cells) as model cancer. In this study, our findings demonstrated that high doses of Lp16-PSP resulted in the induction of morphological changes (Fig. 1A), nuclear chromatin condensation (Fig. 1C), cleavage of chromosomal DNA in a DNA ladder-like pattern (Fig. 1D), accumulation of significant percentage of apoptotic cells in the lower right (Annexin V+/PI-) and upper right (Annexin V+/PI+) quadrants (Fig. 1E) and the loss of mitochondrial membrane potential (Fig. 2D) in HL-60 cells.

Initially, the expression of apoptosis- and cell cycle-related genes was evaluated by qRT-PCR. The results showed that Lp16-PSP treatment (IC_{50} concentration) for 48 h resulted in the upregulation of *Bax*, *caspase-3*, *caspase-8*, *caspase-9*, *FasL*, *p21*, and *p27* with the downregulation of *Bcl-2*, *cdk2*, *cdk4*, *cdk6*, *cyclin D1*, and *cyclin E1* transcripts in HL-60 cells (Fig. 2A, 3B). Activation of the initiator (caspase-8, caspase-9) and the effector caspases (caspase-3) was confirmed by colorimetric analysis, where Lp16-PSP resulted in the dose-dependent increase in the activity of caspase-3, -8 and -9 (Fig. 2B). Increased expression of FasL and activation of caspase-8 clearly demonstrated that extrinsic pathway might be involved in Lp16-PSP induced apoptosis. Furthermore, western blot analysis revealed the cleavage of caspase-3, increased expression of Bax, Bcl-2, and release of cytochrome c after treatment with Lp16-PSP in a dose-dependent fashion (Fig. 2C and 2E). These findings suggested the involvement of intrinsic pathway in Lp16-PSP induced apoptosis in HL-60 cells.

Low doses of Lp16-PSP resulted in the anchorage-independent growth inhibition (Fig. 1B) and the induction of G_1 cell cycle arrest as demonstrated by the results of flow cytometry (Fig. 3A). In addition, increased expression of the universal inhibitor of cyclin-cdk complexes ($p21^{WAF1/CIP1}$) together with the decreased expression of cyclin D, E, and cdk6 was also confirmed by western blot analysis (Fig. 3C). These findings suggest that Lp16-PSP resulted in the induction of $p21^{WAF1/CIP1}$ mediated G_1 cell cycle arrest in HL-60 cells. Several studies have shown that induction of apoptosis and cell cycle arrest are the valuable strategies for cancer drug discovery [37-39]. However, at this stage, it's difficult to conclude the possible molecular mechanism of the action of Lp16-PSP and further support our experimental findings on the basis of previously reported information associated with the other members of YjgF/YER057c/UK114 family. Although antineoplastic, ribonuclease, inhibition of protein synthesis and antiviral activities of the other members of YjgF/YER057c/UK114 protein family has been reported [40-45], and afterward it was proven that translation inhibition was driven by endoribonucleolytic activity. In addition, various ribonucleases have also been reported to have selective anticancer properties [46-50]. Based on previously available information related to YjgF/YER057c/UK114 family members and our findings in this study, we believe that Lp16-PSP might have exerted its *in vitro* anticancer activity through RNA (s) degradation and/or through the inhibition of protein synthesis. However, this study gives a very preliminary indication of the potential application of Lp16-PSP in combating cancer. Thus, further investigations are needed to overcome the shortcomings of this study including the *in vitro* enzymatic (endoribonuclease) activity of Lp16-PSP, substrate/target identification (tRNA, rRNA, mRNA, microRNA or lncRNA), mode of entry into the cell (specific receptors mediated endocytosis), resistance to ribonuclease inhibitors, site of action (nucleus/cytosol), interaction with intracellular molecules, so that the detailed molecular mechanism in both *in vitro* and *in vivo* models can be explored, activity of Lp16-PSP can be compared with the already known antitumor ribonucleases and most important therapeutic implication of Lp16-PSP can be made possible in near future after concrete preclinical and clinical trials.

4. Material and Methods:

Expression of the Recombinant Protein Lp16-PSP: The Latcripin-16 (designated as Lp16-PSP) is one of the registered proteins of *Lentinula edodes* C₉₁₋₃ from our laboratory, with the accession # AHB81541. The expression and recovery of the bioactive form of 32 kDa Lp16-PSP protein were accompanied as described

previously [15]. Briefly, for routine experimentation, Lp16-PSP was expressed at 37 °C after induction with 0.5 mM IPTG for 4 h, in Rosetta gami (DE3), using pET32a (+) as the expression vector. Solubilization of the protein was achieved by mild solubilization buffer containing 2 M urea by the freeze-thaw method. Purification and refolding were done under optimized conditions. The finalized protein thus obtained after extensive dialysis was concentrated by using PEG 20,000. At each step, Lp16-PSP was qualitatively and quantitatively analyzed by SDS-PAGE and BCA respectively and then used subsequently for biological assays.

Human Leukemia HL-60 Cells and Culture Conditions: Human acute promyeloid leukemia cell line (HL-60) was obtained from Shanghai cell bank, Chinese Academy of Sciences (Shanghai, China) and was grown in RPMI medium containing 10% fetal bovine serum, penicillin (100 units/ml) and streptomycin (100 µg/ml) at 37 °C in a humidified atmosphere containing 5 % CO₂. HL-60 cells were maintained in exponential growth, and they were passaged when cell confluency reached ~ 80 %.

Antibodies, Kits, and Reagents: Bax, Bcl-2, caspase-3, cdk6, cytochrome c, cyclin D1, cyclin E1, GAPDH, p21, secondary antibodies and RIPA buffer were from Proteintech (China). The Annexin-V/PI Kit, Mitochondrial membrane potential kit, Hoechst 33258 Assay Kit and DNA fragmentation kit, Caspase-3, -8 and -9 kits were purchased from keyGEN BioTECH (Nanjing, China). The qRT-PCR kit was purchased from Transgene (China). All other reagents and chemicals were purchased from standard commercial sources.

Phase Contrast Imaging: The HL-60 cells (2 × 10⁵ cells/well) after overnight incubation at 37 °C in 12 well plate was washed with PBS once and grown for 48 h in culture media with previously established doses of Lp16-PSP (0 µg/ml, 50 µg/ml, 100 µg/ml and 150 µg/ml). After treatment cell morphology was examined and photographed by using phase contrast microscope [51].

Soft-agar Colony Formation Assay: The evaluation of anchorage-independent growth was done by clonogenicity of cells on soft-agar. Lp16-PSP treated (0 µg/ml, 12.5 µg/ml, 25 µg/ml and 50 µg/ml) HL-60 were mixed with 1.2 % agar in growth medium, and plated on top of a solidified layer of 0.3% agar in growth medium, in 6 well plates. Cells were fed every 3 days with growth medium, and colony formation was observed daily under a phase-contrast microscope. A number of colonies were counted in five fields under a microscope at 40 × magnification [52].

Hoechst 33258 Staining: HL-60 cells (2 × 10⁵ cells/well) in 12 well plate after treatment with indicated concentrations of Lp16-PSP for 48 h were washed twice with cold buffer A provided with the kit (Hoechst 33258 Detection Kit, Keygen, China) and fixed by using 4 % formaldehyde solution at 4 °C for 10 min. Cells were washed again with buffer A and stained with 100 µl of Hoechst 33258 working solution for 10 min at room temperature. After washing with water and air dry, cells were observed with a fluorescence microscope.

DNA Fragmentation Assay: HL-60 cells (5 × 10⁶ cells) were treated with different concentration of Lp16-PSP (0 µg/ml, 50 µg/ml, 100 µg/ml, and 150 µg/ml), and after 48 h of treatment DNA fragmentation assay was done following the manufacturer's instructions (DNA Fragmentation Assay Kit KeyGen, China). Briefly, cells after treatment were collected in 1.5 E.P tubes and washed with PBS. Cells were lysed with

the lysis buffer and enzymes provided with the kit, DNA was then precipitated and washed with 70 % ethanol. 10 μ L of DNA samples were mixed with the loading buffer, run on 1.5 % agarose gel and image was captured by a ChemiDco™ XRS + Imager-Bio-Rad.

Colorimetric Analysis of Caspase-3, -8 and -9: Caspase activities in HL-60 cells after treatment with indicated concentrations of Lp16-PSP for 48 h, were measured by using the commercially available kits (Caspase-3, -8 and -9 Kit KeyGen, China). Briefly, cells after treatment with several concentrations of Lp16-PSP for 48 h, were washed twice with PBS and subjected to caspase assay as per manufacturer's instructions. The activity of the caspase-3, -8 and -9 was normalized and expressed as $O.D_{Test} / O.D_{Control} \times 100$.

Apoptosis Analysis using Annexin-V-FITC/PI Staining: HL-60 cells were treated with different concentrations of Lp16-PSP for 48 h. Thereafter, cells were collected, washed and stained as per manufacturer's instructions (Apoptosis Detection Kit Keygen, China). The rate of apoptosis was measured by flow cytometry (FACS-Calibur Cytometer (BD Biosciences, Heidelberg, Germany)) within 1 h.

Mitochondrial Membrane Potential ($\Delta\psi_m$) Measurement using JC-1 staining by Flow Cytometry: Mitochondrial membrane potential assay was performed as per manufacturer's instructions. Briefly, HL-60 cells after treatment with Lp16-PSP (0 μ g/ml, 100 μ g/ml, and 150 μ g/ml) for 48 h were collected after centrifugation and washed twice with PBS. Cells were then incubated with the working solution of JC-1 stain at 37 °C for 30 min. Cells were then collected and resuspended in incubation buffer provided with the kit, and loss of mitochondrial membrane potential was analyzed by using a FACS-Calibur Cytometer (BD Biosciences, Heidelberg, Germany).

Cell-Cycle Analysis by Flow Cytometry: HL-60 cells were treated with indicated concentrations of Lp16-PSP for 48 h. After treatment cells were collected, washed with PBS and fixed overnight with 70 % ethanol at 4 °C. After fixing, cells were collected by slow centrifugation, washed with ice-cold PBS and resuspended at a concentration of 1×10^6 cells/ml in 5 μ g/ml RNase and 50 μ g/ml propidium iodide. The cells were then incubated for 30 min at 37 °C and analyzed by using a FACS-Calibur Cytometer (BD Biosciences, Heidelberg, Germany).

Isolation of RNA and Quantitative Real-Time Polymerase Chain Reaction (qRT-PCR): Expression of the apoptosis- and cell cycle-related genes was determined by quantitative real-time PCR. After treatment of the HL-60 cells with IC_{50} concentration for 48 h, total RNA was extracted from Lp16-PSP treated and control cells with TRIzol reagent (Life Technology), according to the manufacturers' instructions. One microgram of RNA was used to generate cDNA by using Transgene RT reagent Kit with gDNA remover. To quantify a number of transcripts, SYBER Green based qPCR was performed with RT master mix (Transgene) using Real-Time PCR System (StepOne™). The thermal profile used was as follows: For Reverse transcription 42 °C - 15 min, 85 °C - 5 s, for quantitative PCR 94 °C - 30 s, 40 x [94 °C - 5 s, 60 °C - 15 s, 72 °C - 10 s]. The primer sequences for apoptosis- and cell cycle-related genes are listed in (Table.1). GAPDH was used as internal control and all the reactions were performed in triplicate. The relative gene expression was calculated by using the $2^{-\Delta\Delta C_T}$ method as described previously [53].

Table 1: qRT-PCR Primer Sequences

Gene (s)	Forward 5' → 3'	Reverse 5' → 3'
<i>Bax</i>	CCCGAGAGGTCTTTTCCGAG	CCAGCCCATGATGGTTCTGAT
<i>Bcl-2</i>	GGTGGGGTCATGTGTGTGG	CGGTTCAGGTACTCAGTCATCC
<i>Cas3</i>	AGAGGGGATCGTTGTAGAAGTC	ACAGTCCAGTTCTGTACCACG
<i>Cas8</i>	TTTCTGCCTACAGGGTCATGC	TGTCCAACCTTTCCTTCTCCCA
<i>Cas9</i>	CTCAGACCAGAGATTCGCAAAC	GCATTTCCTCTCAAACCTCTCAA
<i>Cdk2</i>	GCCATTCTCATCGGGTCCTC	ATTTCAGCCCAGGAGGATT
<i>Cdk4</i>	ATGGCTACCTCTCGATATGAGC	CATTGGGGACTCTCACACTCT
<i>Cdk6</i>	CTGCAGGGAAAGAAAAGTGC	CTCCTCGAAGCGAAGTCCTC
<i>Cyclin D1</i>	GCTGCGAAGTGGAACCAT	CCTCCTTCTGCACACATTGAA
<i>Cyclin E1</i>	AAGGAGCGGGACACCATGA	ACGGTCACGTTTGCTTCC
<i>FasL</i>	TGCCTTGGTAGGATTGGGC	GCTGGTAGACTCTCGAGTTC
<i>GAPDH</i>	AATCCCATCACCATCTTCCA	TGGACTCCACGACGTACTCA
<i>p21</i>	TGTCCGTCAGAACCCATGC	AAAGTCGAAGTTCCATCGCTC
<i>p27</i>	TAATTGGGGCTCCGGCTAACT	TGCAGGTCGCTTCCTTATTCC

Western Blotting: Lp16-PSP treated and control cells were lysed in RIPA buffer supplemented with protease inhibitors. Cell lysates were cleared by centrifugation at 14,000 rpm, for 20 min at 4 °C and proteins (20 – 40 µg) were resolved by electrophoresis and transferred to polyvinylidene fluoride (PVDF) membranes. In order to prevent the non-specific antibody binding, membranes were blocked with blocking buffer (5 % skimmed milk in TBS-T (20 mM Tris-HCl (pH 7.5), 150 mM NaCl, 0.1 % Tween 20)) at room temperature for 1 h. Blots were incubated at 4 °C overnight with the following antibodies diluted with blocking buffer: Bax (Cat # 23931-1-AP, 1:500), Bcl-2 (Cat # 12789-1-AP, 1:1000), caspase-3 (Cat # 19677-1-AP, 1:200), cyclin D1 (Cat # 60186-1-AP, 1:2000), cyclin E1 (Cat # 11554-1-AP, 1:500), cdk6 (Cat # 14052-1-AP, 1:200), cytochrome c (Cat # 10993-1-AP, 1:200), GAPDH (Cat # 23931-1-AP, 1:500), p21 (Cat # 10355-1-AP, 1:500). Next membranes were incubated with the Second antibodies: Goat anti-rabbit IgG, Goat anti-mouse IgG (HRP-conjugated, Proteintech) (Cat # 23931-1-AP, SA00001-1, 1:500) at room temperature for 1 h. Blots were developed with ECL chemiluminescence detection kit and images were captured by a ChemiDco™ XRS + Imager-Bio-Rad.

Statistical Evaluation: Statistical analysis was done by using GraphPad Prism 5.0 software (La Jolla, CA, USA). All the experiments were done in triplicate unless otherwise stated. Data were evaluated for significance by using one-way analysis of variance (ANOVA) followed by Tukey’s Multiple Comparison Test.

Acknowledgments: This work was supported by Chinese Government Scholarship (CSC No: 2014GXY960). We would like to express our gratitude to Richardson Patrick Joseph for editorial assistance and Shao LiQun and FangYu Kun for their generous technical support.

Author Contributions: Thomson Patrick Joseph and Warren Chanda have participated in the design of the study, performed all the experiments and prepared the manuscript. Abdullah Faqeer Muhammad and Sadia Kanwal have contributed reagents and analyzed the data. Samana Batool and Zhang Meishan have contributed in revising the manuscript. MinTao Zhong has contributed in the interpretation of the results and revision of the manuscript. Min Huang was responsible for the final approval of the manuscript for publication.

Conflict of interest: The authors declare no conflict of interest.

References:

1. Siegel, R.L.; Miller, K.D.; Jemal, A. Cancer statistics, 2017. *CA: A Cancer Journal for Clinicians* 2017, 67, 7-30.
2. Hamilton, M.R.H.a.P.J. Haematology: An illustrated colour text. 2002, 2nd edition.

- 408 3. Recher, C.; Beyne-Rauzy, O.; Demur, C.; Chicanne, G.; Dos Santos, C.; Mas, V.M.; Benzaquen,
409 D.; Laurent, G.; Huguet, F.; Payrastre, B. Antileukemic activity of rapamycin in acute myeloid
410 leukemia. *Blood* 2005, **105**, 2527-2534.
- 411 4. Coombs, C.C.; Tavakkoli, M.; Tallman, M.S. Acute promyelocytic leukemia: Where did we start,
412 where are we now, and the future. *Blood cancer journal* 2015, **5**, e304.
- 413 5. Sanz, M.A.; Lo Coco, F.; Martin, G.; Avvisati, G.; Rayon, C.; Barbui, T.; Diaz-Mediavilla, J.;
414 Fioritoni, G.; Gonzalez, J.D.; Liso, V., *et al.* Definition of relapse risk and role of
415 nonanthracycline drugs for consolidation in patients with acute promyelocytic leukemia: A
416 joint study of the pethema and gimema cooperative groups. *Blood* 2000, **96**, 1247-1253.
- 417 6. Tallman, M.S.; Andersen, J.W.; Schiffer, C.A.; Appelbaum, F.R.; Feusner, J.H.; Ogden, A.;
418 Shepherd, L.; Willman, C.; Bloomfield, C.D.; Rowe, J.M., *et al.* All-trans-retinoic acid in acute
419 promyelocytic leukemia. *The New England journal of medicine* 1997, **337**, 1021-1028.
- 420 7. Kinghorn, A. Foye's principles of medicinal chemistry. Lemke, t.; williams, da., editors.
421 Baltimore: Wolters kluwer/lippincott williams & wilkins. 2008, 12-25.
- 422 8. Lucas, D.M.; Still, P.C.; Perez, L.B.; Grever, M.R.; Kinghorn, A.D. Potential of plant-derived
423 natural products in the treatment of leukemia and lymphoma. *Current drug targets* 2010, **11**,
424 812-822.
- 425 9. Saedi, T.A.; Md Noor, S.; Ismail, P.; Othman, F. The effects of herbs and fruits on leukaemia.
426 *Evidence-Based Complementary and Alternative Medicine* 2014, **2014**, 8.
- 427 10. Gurova, K. New hopes from old drugs: Revisiting DNA-binding small molecules as anticancer
428 agents. *Future oncology (London, England)* 2009, **5**, 1685-1704.
- 429 11. D'Errico, G.; Ercole, C.; Lista, M.; Pizzo, E.; Falanga, A.; Galdiero, S.; Spadaccini, R.; Picone, D.
430 Enforcing the positive charge of n-termini enhances membrane interaction and antitumor
431 activity of bovine seminal ribonuclease. *Biochimica et biophysica acta* 2011, **1808**, 3007-3015.
- 432 12. Fang, E.F.; Zhang, C.Z.; Zhang, L.; Fong, W.P.; Ng, T.B. In vitro and in vivo anticarcinogenic
433 effects of rnase mc2, a ribonuclease isolated from dietary bitter melon, toward human liver
434 cancer cells. *The international journal of biochemistry & cell biology* 2012, **44**, 1351-1360.
- 435 13. Fang, E.F.; Zhang, C.Z.; Fong, W.P.; Ng, T.B. Rnase mc2: A new momordica charantia
436 ribonuclease that induces apoptosis in breast cancer cells associated with activation of mapks
437 and induction of caspase pathways. *Apoptosis : an international journal on programmed cell*
438 *death* 2012, **17**, 377-387.
- 439 14. Lomax, J.E.; Eller, C.H.; Raines, R.T. Rational design and evaluation of mammalian ribonuclease
440 cytotoxins. *Methods in enzymology* 2012, **502**, 273-290.
- 441 15. Thomson Patrick Joseph, W.C. Expression and selective in vitro anticancer activity of lp16-psp,
442 a member of yjgf/yer057c/uk114 protein family from the mushroom lentinula edodes c91-
443 3.(Submitted).
- 444 16. Anoikis resistance: An essential prerequisite for tumor metastasis. *International Journal of Cell*
445 *Biology* 2012, **2012**.
- 446 17. Zhang, X.; Zhong, L.; Liu, B.Z.; Gao, Y.J.; Gao, Y.M.; Hu, X.X. Effect of gins2 on proliferation and
447 apoptosis in leukemic cell line. *International journal of medical sciences* 2013, **10**, 1795-1804.
- 448 18. Galluzzi, L.; Vitale, I.; Abrams, J.M.; Alnemri, E.S.; Baehrecke, E.H.; Blagosklonny, M.V.;
449 Dawson, T.M.; Dawson, V.L.; El-Deiry, W.S.; Fulda, S., *et al.* Molecular definitions of cell death
450 subroutines: Recommendations of the nomenclature committee on cell death 2012. *Cell death*
451 *and differentiation* 2012, **19**, 107-120.
- 452 19. Balasubramanian, K.; Mirnikjoo, B.; Schroit, A.J. Regulated externalization of
453 phosphatidylserine at the cell surface: Implications for apoptosis. *The Journal of biological*
454 *chemistry* 2007, **282**, 18357-18364.

- 455 20. Wyllie, A.H. Glucocorticoid-induced thymocyte apoptosis is associated with endogenous
456 endonuclease activation. *Nature* 1980, **284**, 555-556.
- 457 21. Zhang, J.H.; Xu, M. DNA fragmentation in apoptosis. *Cell Res* 2000, **10**, 205-211.
- 458 22. Arora, S.; Tandon, S. DNA fragmentation and cell cycle arrest: A hallmark of apoptosis induced
459 by ruta graveolens in human colon cancer cells. *Homeopathy* 2015, **104**, 36-47.
- 460 23. Lee, S.H.; Meng, X.W.; Flatten, K.S.; Loegering, D.A.; Kaufmann, S.H. Phosphatidylserine
461 exposure during apoptosis reflects bidirectional trafficking between plasma membrane and
462 cytoplasm. *Cell death and differentiation* 2013, **20**, 64-76.
- 463 24. Susin, S.A.; Daugas, E.; Ravagnan, L.; Samejima, K.; Zamzami, N.; Loeffler, M.; Costantini, P.;
464 Ferri, K.F.; Irinopoulou, T.; Prevost, M.C., *et al.* Two distinct pathways leading to nuclear
465 apoptosis. *The Journal of experimental medicine* 2000, **192**, 571-580.
- 466 25. Galluzzi, L.; Vitale, I.; Abrams, J.M.; Alnemri, E.S.; Baehrecke, E.H.; Blagosklonny, M.V.;
467 Dawson, T.M.; Dawson, V.L.; El-Deiry, W.S.; Fulda, S., *et al.* Molecular definitions of cell death
468 subroutines: Recommendations of the nomenclature committee on cell death 2012. *Cell death*
469 *and differentiation* 2012, **19**, 107-120.
- 470 26. Zapata, J.M.; Pawlowski, K.; Haas, E.; Ware, C.F.; Godzik, A.; Reed, J.C. A diverse family of
471 proteins containing tumor necrosis factor receptor-associated factor domains. *The Journal of*
472 *biological chemistry* 2001, **276**, 24242-24252.
- 473 27. Hockenbery, D.; Nunez, G.; Millman, C.; Schreiber, R.D.; Korsmeyer, S.J. Bcl-2 is an inner
474 mitochondrial membrane protein that blocks programmed cell death. *Nature* 1990, **348**, 334-
475 336.
- 476 28. Riedl, S.J.; Shi, Y. Molecular mechanisms of caspase regulation during apoptosis. *Nature*
477 *reviews. Molecular cell biology* 2004, **5**, 897-907.
- 478 29. Gross, A.; McDonnell, J.M.; Korsmeyer, S.J. Bcl-2 family members and the mitochondria in
479 apoptosis. *Genes & development* 1999, **13**, 1899-1911.
- 480 30. Naseri, M.H.; Mahdavi, M.; Davoodi, J.; Tackallou, S.H.; Goudarzvand, M.; Neishabouri, S.H.
481 Up regulation of bax and down regulation of bcl2 during 3-nc mediated apoptosis in human
482 cancer cells. *Cancer cell international* 2015, **15**, 55.
- 483 31. Green, D.R.; Kroemer, G. The pathophysiology of mitochondrial cell death. *Science (New York,*
484 *N.Y.)* 2004, **305**, 626-629.
- 485 32. Sherr, C.J.; Roberts, J.M. Cdk inhibitors: Positive and negative regulators of g1-phase
486 progression. *Genes & development* 1999, **13**, 1501-1512.
- 487 33. Sherr, C.J.; Roberts, J.M. Inhibitors of mammalian g1 cyclin-dependent kinases. *Genes &*
488 *development* 1995, **9**, 1149-1163.
- 489 34. Sherr, C.J. G1 phase progression: Cycling on cue. *Cell* 1994, **79**, 551-555.
- 490 35. Grana, X.; Reddy, E.P. Cell cycle control in mammalian cells: Role of cyclins, cyclin dependent
491 kinases (cdks), growth suppressor genes and cyclin-dependent kinase inhibitors (ckis).
492 *Oncogene* 1995, **11**, 211-219.
- 493 36. Kastan, M.B.; Canman, C.E.; Leonard, C.J. P53, cell cycle control and apoptosis: Implications for
494 cancer. *Cancer metastasis reviews* 1995, **14**, 3-15.
- 495 37. Zhang, L.; Zheng, Y.; Deng, H.; Liang, L.; Peng, J. Aloperine induces g2/m phase cell cycle arrest
496 and apoptosis in hct116 human colon cancer cells. *International journal of molecular medicine*
497 2014, **33**, 1613-1620.
- 498 38. Zhang, M.H.; Man, H.T.; Zhao, X.D.; Dong, N.; Ma, S.L. Estrogen receptor-positive breast cancer
499 molecular signatures and therapeutic potentials (review). *Biomedical reports* 2014, **2**, 41-52.
- 500 39. Zhang, J.; Wei, W.; Jin, H.C.; Ying, R.C.; Zhu, A.K.; Zhang, F.J. Programmed cell death 2 protein
501 induces gastric cancer cell growth arrest at the early s phase of the cell cycle and apoptosis in
502 a p53-dependent manner. *Oncology reports* 2015, **33**, 103-110.

40. Oka, T.; Tsuji, H.; Noda, C.; Sakai, K.; Hong, Y.M.; Suzuki, I.; Munoz, S.; Natori, Y. Isolation and characterization of a novel perchloric acid-soluble protein inhibiting cell-free protein synthesis. *The Journal of biological chemistry* 1995, **270**, 30060-30067.
41. Colombo, I.; Cecilian, F.; Ronchi, S.; Bartorelli, A.; Berra, B. Cdna cloning and escherichia coli expression of uk114 tumor antigen. *Biochimica et biophysica acta* 1998, **1442**, 49-59.
42. Morishita, R.; Kawagoshi, A.; Sawasaki, T.; Madin, K.; Ogasawara, T.; Oka, T.; Endo, Y. Ribonuclease activity of rat liver perchloric acid-soluble protein, a potent inhibitor of protein synthesis. *The Journal of biological chemistry* 1999, **274**, 20688-20692.
43. A. Bartorelli, G.Z., F. Fassio, M. Botta, R. Ferrara,; M. Bailo, C.B., V. Cavalca, C. Arzani, R. Maraschin,. Toxicological and antitumoral activity of uk101, a mammalian liver extract, . *J. Tumor Marker Oncol.* 1994, **9**.
44. Ghezzi, F.; Berta, G.N.; Bussolati, B.; Bosio, A.; Corvetto, G.; Di Carlo, F.; Bussolati, G.; Guglielmone, R.; Bartorelli, A. Perchloric acid-soluble proteins from goat liver inhibit chemical carcinogenesis of syrian hamster cheek-pouch carcinoma. *Br J Cancer* 1999, **79**, 54-58.
45. S. Racca, F.D.C., A. Bartorelli, B. Bussolati, G. Bussolati. Growth inhibition of dmbs-induced rat mammary carcinomas by uk114 treatment,. *Virchows Arch* 1997, **431**, 323-328.
46. Ardelt, B.; Ardelt, W.; Pozarowski, P.; Kunicki, J.; Shogen, K.; Darzynkiewicz, Z. Cytostatic and cytotoxic properties of amphinase: A novel cytotoxic ribonuclease from rana pipiens oocytes. *Cell cycle (Georgetown, Tex.)* 2007, **6**, 3097-3102.
47. Ardelt, W.; Shogen, K.; Darzynkiewicz, Z. Onconase and amphinase, the antitumor ribonucleases from rana pipiens oocytes. *Current pharmaceutical biotechnology* 2008, **9**, 215-225.
48. Castro, J.; Ribo, M.; Navarro, S.; Nogues, M.V.; Vilanova, M.; Benito, A. A human ribonuclease induces apoptosis associated with p21waf1/cip1 induction and jnk inactivation. *BMC cancer* 2011, **11**, 9.
49. Zhang, R.; Zhao, L.; Wang, H.; Ng, T.B. A novel ribonuclease with antiproliferative activity toward leukemia and lymphoma cells and hiv-1 reverse transcriptase inhibitory activity from the mushroom, hohenbuehelia serotina. *International journal of molecular medicine* 2014, **33**, 209-214.
50. Vert, A.; Castro, J.; Ribo, M.; Benito, A.; Vilanova, M. A nuclear-directed human pancreatic ribonuclease (pe5) targets the metabolic phenotype of cancer cells. *Oncotarget* 2016, **7**, 18309-18324.
51. Lu, C.C.; Yang, J.S.; Huang, A.C.; Hsia, T.C.; Chou, S.T.; Kuo, C.L.; Lu, H.F.; Lee, T.H.; Wood, W.G.; Chung, J.G. Chrysophanol induces necrosis through the production of ros and alteration of atp levels in j5 human liver cancer cells. *Molecular nutrition & food research* 2010, **54**, 967-976.
52. Kim, A.; Im, M.; Yim, N.H.; Ma, J.Y. Reduction of metastatic and angiogenic potency of malignant cancer by eupatorium fortunei via suppression of mmp-9 activity and vegf production. *Scientific reports* 2014, **4**, 6994.
53. Schmittgen, T.D.; Livak, K.J. Analyzing real-time pcr data by the comparative ct method. *Nat. Protocols* 2008, **3**, 1101-1108.